Novel $Zn_xSn_{1-x}Se$ Absorber For Use in Thin-Film Solar Cells

T.M.Razykov[1], E. Artegiani[2], G.S. Boltaev[3], A.Bosio[4], B.Ergashev[1], K.M.Kouchkarov[1], N.K. Mamarasulov[1]
A.A. Mavlonov[1], A.Romeo[2], N.Romeo[4], R.Yuldoshov[1]

[1]Physical-Technical Institute, Uzbekistan Academy of Science,
Bodomzor Yoli 2B, Tashkent 100084, Uzbekistan
Phone: +998-71-235-4103, Fax: +998-71-235-4291, E-mail: razykov@uzsci.net
[2]Universita' di Verona, Ca' Vignal 2- Strada Le Grazie 15, 37134 Verona, Italy
[3]Ion Plasma and Laser Technologies, Uzbek Academy of Sciences, Tashkent 100125, Uzbekistan
[4]University of Parma, G.P Usberti 7/A - 43124 Parma, Italy

ABSTRACT

$Zn_xSn_{1-x}Se$ (x=0) thin films were fabricated by chemical vapor deposition (CVD) using polycrystalline tin selenide (SnSe) precursors. The morphology, structure, optical and electrical properties of films were studied as a function of the composition of precursors and the substrate temperature. Results obtained have shown that Se rich films were fabricated at low substrate temperatures, despite the different compositions of the SnSe precursor during the synthesis. In this case, the grain sizes of the films vary in the range of 8-20 μm, depending on the substrate temperature. X-ray diffraction (XRD) analysis of the samples showed that the films have a orthorhombic crystalline structure. The optical measurements have revealed that the samples have optical bandgap of 1.21 eV and the absorption coefficient of $\sim 10^5$ cm^{-1}. The samples performed p-type conductivity being in the range of 10-10^2 (Ohm×cm)$^{-1}$ depending on the deposition conditions.

Keywords: $Zn_xSn_{1-x}Se$, CVD, thin film, bandgap.

1. INTRODUCTION

Today the leading materials in the world photovoltaic market are Si wafers, Cu(In,Ga)Se$_2$ (CIGS) and CdTe thin films. Currently, remarkable efficiencies were achieved on these cells, i.e. Si (26.0 %), CIGS (22.6 %) and CdTe (22.1 %). However, these materials have serious disadvantages: Si has low absorption coefficient and wafer form, CIGS contains high cost materials (In and Ga) and CdTe has a toxicity issue of Cd and limited resources of Te. While novel, very promising $Zn_xSn_{1-x}Se$ thin films have ideal properties for fabrication of low cost and high efficiency thin film solar cells for large scale terrestrial application: 1) high absorption coefficient of $\sim 10^5$ cm^{-1}, 2) band gap of 0.9-2.7 eV which allows fabrication of single (1.46 eV) and double junction (1.0 eV and 1.7 eV) cells, and 3) the conductivity can be varied in very wide range of 10-10^2 (Ohm×cm)$^{-1}$ which means that doping to reduce the series resistance is not necessary, since the conductivity can be varied by the controlling of the intrinsic point defects. Moreover, it is formed by abundant and environmental-friendly elements. Variety of techniques have been used for the deposition of SnSe films, such as vacuum evaporation [1], chemical bath deposition [2], electro-deposition [3], solid state reactions [4], solvothermal [5], molecular beam epitaxy [6], pulsed laser deposition [7] and chemical vapor deposition [8].

Moreover, this material is promising for applications in many fields, such as solar cells [9–11], thin film light emitting diodes (LED) [11], low threshold lasers, optical amplifiers for telecommunication networks [12], guided wave devices, chemical and biosensors [13].

In this work, effect of the stoichiometric, Sn rich and Se rich precursors on structural, morphological, optical and electrical properties of SnSe films is discussed for the first time.

2. EXPERIMENTAL

The stoichiometric, Sn rich and Se rich granules with 99.999 % purity were used as precursors. The temperature of the precursors was varied in the range of 850℃-950℃. The temperature of the substrate was varied between 450℃ - 550℃. The flow rate of the carrier gas was ~ 20 cm^3/min. The duration of the deposition process depends on the required film thickness and ranges between 30-60 min. All SnSe thin films have been grown on borosilicate glasses. The crystal structure and the phase of the material compositions were studied by XRD using a "Panalytical Empyrean" diffractometer (Cu Kα radiation, λ = 1.5418 Å) with a wide-angle measurements of 2θ in the range of 20°-80° and a step of 0.010. The experimental data were analyzed using the Joint Committee on Powder Diffraction Standard (JCPDS). Morphological studies were carried out using a scanning electron microscope (SEM-EVO MA 10), and film compositions were determined using an energy-dispersive X-ray spectroscopy (EDX, Oxford Instrument - Aztec Energy Advanced X-act SDD). Optical parameters of selected SnSe thin films were determined from the transmission spectra obtained in a wide spectral range between 400-2500 nm using the HR 4000 Ocean Optic spectrometer with a resolution of 2 nm. Silver was used as ohmic contact for the p-type films. The type of conductivity of the samples was determined by thermoelectric effect. The thickness of the films was determined by using microinterferometer MII-4, and the method of precision micro-weighting (on FA 120 4C scales with an accuracy of 0.1 mg).

3. RESULTS AND DISCUSSIONS

According to EDX data, the obtained films have no any impurity elements within the sensitivity of the method (Fig. 1). The deposited films from the Sn rich SnSe precursor have

Sn$_{0.98}$Se T=450°C
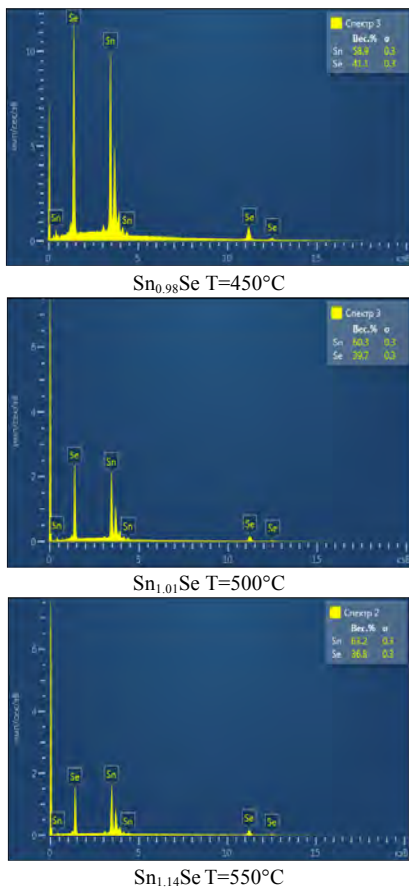

Sn$_{1.01}$Se T=500°C

Sn$_{1.14}$Se T=550°C

Figure 1 Results of energy dispersive X-ray spectroscopy analysis for SnSe thin films deposited from Sn enriched precursor at indicated substrate temperatures.

almost similar as stoichiometric precursor at substrate temperatures of 450℃ and 500℃. On the other hand, the film grown at 550℃ has Sn rich composition. This can be explained by the fact that when the substrate temperature increases, Se re-evaporates from the substrate, which results in enrichment of the Sn in the films. All films deposited from the SnSe precursors, i.e. Se enriched and with stoichiometric composition, have Se enriched composition at different temperatures (Table 1). All SnSe films studied in this work have a smooth surface without cracks and pores on the surface of the substrate. Figure 2 shows the XRD patterns of SnSe films deposited from three different SnSe precursors, i.e. Sn enriched, Se enriched and with stoichiometric composition, for three different substrate temperatures. According to XRD analysis, all samples have single-phase, the orthorhombic structure of SnSe and there are no other crystalline phases of Sn, Se, Sn$_2$Se$_3$, SnSe$_2$, SnO$_2$, etc. The main peaks are corresponding to the (400) and (111) preferential orientation of SnSe (Fig. 2). A similar results were also noted in several papers devoted to SnSe films obtained by thermal evaporation and chemical vapor deposition [8].

The authors conducted this, presence of both (400) and (111) preferential orientations to the growth conditions, e.g. substrate temperature, the distance between the substrate and the target. In this work, (111) plane was observed only for SnSe thin films deposited from Sn enriched SnSe precursor at 550℃ (Fig. 2a). Analyzing the XRD data of all samples with a database (JCPDS: 01-089-0233) showed that all films have an orthorhombic structure.

The lattice parameters of the crystal for all samples were calculated using the following formula: $1 / d^2 = h^2 / a^2 + k^2 / b^2 + l^2 / c^2$, where d is the distance between the planes, h, k, l are Miller indices and a, b, c are lattice constants. The lattice constants for thin films deposited at different substrate temperatures from Sn and Se enriched and stoichiometric SnSe precursors have the following values: a = 11.52 Å, b = 4.16 Å, c = 4.43 Å and a = 11.48 Å, b = 4.17 Å, c = 4.39 Å, respectively. These values are in good agreement with the JCPDS database, as well as the data presented in the literature for SnSe thin films grown by various methods [14, 15].

Fig. 3 illustrates SEM images for all samples grown at different substrate temperatures from the Sn and Se enriched as well as stoichiometric SnSe precursors. Although the microcrystals for all SnSe films are uniformly distributed over the film surface, the microstructure (shape and grain size) of the samples depends on the substrate temperature and the precursor composition. With increasing the substrate temperature, the shape of the grains changes, whereas the grain sizes do not change significantly for the films deposited from Sn enriched SnSe precursor (Fig. 3a), and vice versa for the samples obtained from Se enriched and stoichiometric SnSe precursors. Furthermore, the grain shapes of all the samples have a flattened appearance for all substrate temperatures, except for films obtained from Sn enriched in SnSe compound at a substrate temperature of 550℃, which has the form of a parallelepiped.

Table 1 Results of energy dispersive X-ray spectroscopy analysis for SnSe thin films deposited from Se enriched and stoichiometric SnSe precursors

T$_n$(°C)	SnSe thin films deposited from stoichiometric SnSe precursor			SnSe thin films deposited from Se enriched SnSe precursor		
	Composition of the film	Sn%	Se%	Composition of the film	Sn%	Se%
450	Sn$_{0.91}$Se	57.8	42.2	Sn$_{0.89}$Se	57.3	42.7
500	Sn$_{0.91}$Se	57.8	42.2	Sn$_{0.96}$Se	59.2	40.8

550	$Sn_{0.92}Se$	58.2	41.8	$Sn_{0.95}Se$	58.7	41.3

a)   b)   c)
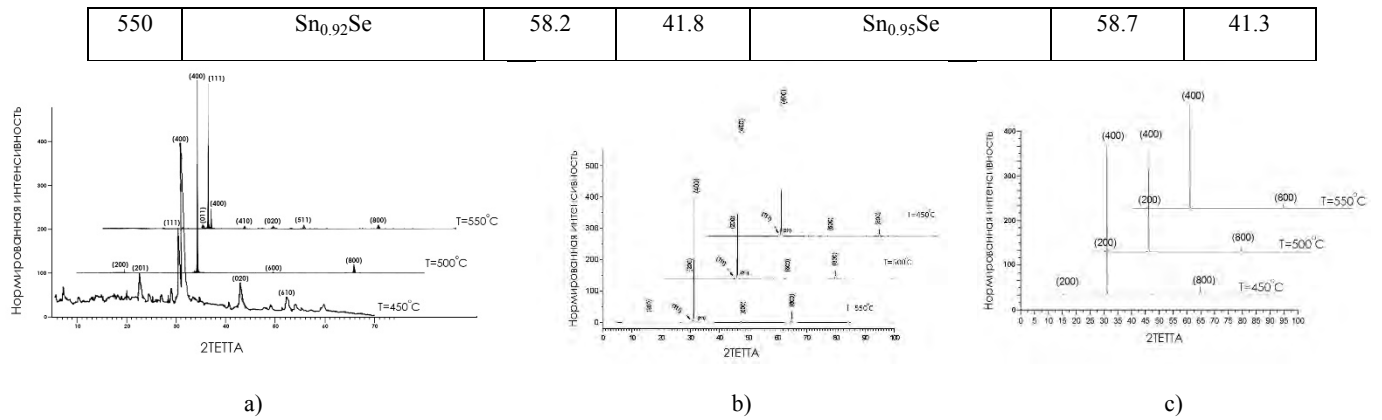
Figure 2. Wide-angle X-ray data of SnSe films obtained from a) Sn enriched, b) stoichiometric and c) Se enriched SnSe precursors at three different substrate temperatures.

Table 2. Electrical parameters of SnSe films. T_s-substrate temperature, σ-electrical conductivity, E_{ac}-activation energy.

T_s (°C)	SnSe thin films deposited from Sn enriched SnSe precursor				SnSe thin films deposited from stoichiometric SnSe precursor				SnSe thin films deposited from Se enriched SnSe precursor			
	Composition of the film	σ (Ohm·cm)$^{-1}$	E_{ac} (eV)	Type of cunductivity	Composition of the film	σ (Ohm·cm)$^{-1}$	E_{ac} (eV)	Type of cunductivity	Composition of the film	σ (Ohm·cm)$^{-1}$	E_{ac} (eV)	Type of cunductivity
450	$Sn_{0.98}Se$	90	0.0023	p	$Sn_{0.91}Se$	6,5	0.0023	p	$Sn_{0.89}Se$	5,5		p
500	$Sn_{1.01}Se$	70	0.0024	p	$Sn_{0.91}Se$	24	0.0025	p	$Sn_{0.96}Se$	20		p
550	$Sn_{1.14}Se$	15	0.0406	p	$Sn_{0.92}Se$	27	0.0026	p	$Sn_{0.95}Se$	24		p

The samples obtained from Sn enriched precursor have similar grain sizes of 8-10 μm and have a polycrystalline structure for all substrate temperatures. However, the grain sizes of the films deposited from Se enriched and stoichiometric SnSe precursors increased, i.e. 8-20 μm, at the substrate temperature of 550 ℃ and the structure become more densely packed. Moreover, disappearance of vertically deposited grains on the surface of all SnSe films was observed with increasing the substrate temperature.

The optical properties of selected SnSe film, i.e. deposited from stoichiometric SnSe precursor at 450 ℃, were studied to determine the absorption coefficient (α) and the optical bandgap (Fig. 4 and 5). As shown, SnSe thin film has the absorption coefficient of ~10^5 cm^{-1} and the optical bandgap of 1.21 eV. These values are in good agreement with [15].

The electrical parameters of the SnSe films, e.g. conductivity σ, activation energy E_{ac} and the type of conductivity, are given in Table 2. As shown, all SnSe thin films illustrate p-type conductivity. The electrical conductivity of SnSe films deposited from Sn enriched SnSe precursor decreases with increasing the substrate temperature. This is explained by increasing the Sn content in the film deposited at high substrate temperature. Unlike, the electrical conductivity of those samples obtained from Se enriched and stoichiometric SnSe precursors increases with increasing the substrate temperature. This improvement is associated with an increase in the grain size and a decrease in the grain boundary density of the films grown at higher substrate temperatures.

4. SUMMARY

We have studied the morphology, structure, optical and electrical properties of SnSe films fabricated at different substrate temperatures and compositions of precursors. It has been found that: 1) at low substrate temperatures, SnSe thin films are Se enriched, i.e. independent of the initial precursor composition; 2) with increasing the substrate temperature, foreign particles disappear from the film surfaces and the films are more closely packed polycrystalline structure; 3) the films have an orthorhombic structure and are characterized by preferential (400) and (111) plane orientations; 4) the electrical conductivity of the SnSe films deposited from Sn enriched precursor decreases with increasing the substrate temperature, whereas increases in SnSe films obtained from the Se enriched and stoichiometric SnSe precursors. Optical measurements showed that the SnSe thin films have a direct band gap of 1.21 eV and a high absorption coefficient of ~ 10^5 cm^{-1}.The samples performed p-type high conductivity of

Sn$_{0.98}$Se T = 450°C   Sn$_{1.01}$Se T = 500°C   Sn$_{1.14}$Se T = 550°C

a)

Sn$_{0.91}$Se T = 450°C   Sn$_{0.91}$Se T = 500°C   Sn$_{0.92}$Se T = 550°C

b)

Sn$_{0.89}$Se T = 450°C   Sn$_{0.96}$Se T = 500°C   Sn$_{0.95}$Se T = 550°C
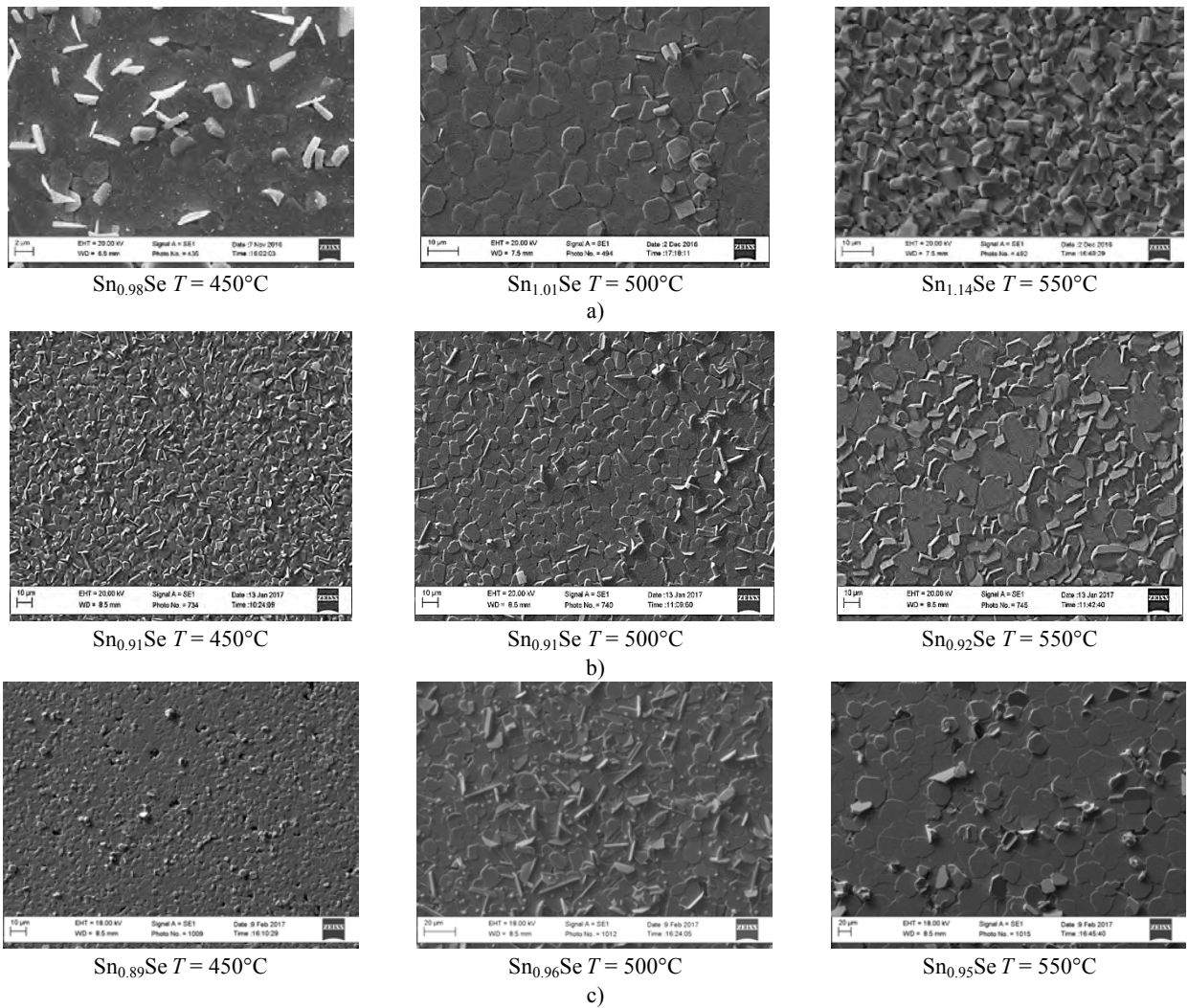
c)

Figure 3. SEM images of SnSe thin films deposited from a) Sn enriched, b) stoichiometric and c) Se enriched SnSe precursors at indicated substrate temperatures.

10-10^2 (Ohm×cm)$^{-1}$ depending on the deposition conditions. Our next step will be fabrication of Zn$_x$Sn$_{1-x}$Se films in the whole range of compositions of $0 \leq x \leq 1$.
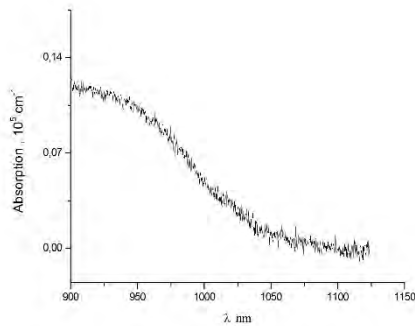

Figure 4. Absorption coefficient as a function of wavelength for SnSe thin film deposited from stoichiometric SnSe precursor at 450 °C.
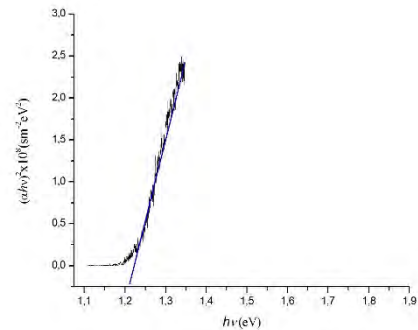
Figure 5. Absorption coefficient versus photon energy for SnSe thin film deposited from stoichiometric SnSe precursor at 450 °C.

5   REFERENCES

[1] D. Pathinettam Padiyan, A. Marikani, K.R. Murali, Electrical and Photoelectrical Properties of Vacuum Deposited SnSe Thin Films, Cryst. Res. Technol. 35 (2000) 949-957.

[2] Z. Zainal, N. Saravanan, K. Anuar, M.Z. Hussein, W.M.M. Yunus, Chemical bath deposition of tin selenide thin films, Mater. Sci. Eng., B, Solid-State Mater. Adv. Technol. 107 (2004) 181-185.

[3] B. Subramanian, T. Mahalingam, C. Sanjeeviraja, M. Jayachandran, M.J. Chockalingam, Electrodeposition of Sn, Se, SnSe and the material properties of SnSe films, Thin Solid Films 357 (1999) 119-124.

[4] D. Tran Quan, SnSe Thin Films Synthesized by Solid State Reactions, Thin Solid Films 149 (1987) 197-203.

[5] Y. Xie, H. Su, B. Li, Y. Qian, A direct solvothermal route to nanocrystalline selenides at low temperature, Mater. Res. Bull. 35 (2000) 459-464.

[6] I.R. Nuriev, E.Y. Salaev, A.K. Sharifova, Ser. Fiz.-Tekh. Mat. Nauk 3 (1982) 91.

[7] R. Teghil, A. Santagata, V. Marotta, S. Orlando, G. Pizzella, A. Giardini-Guidoni, A. Mele, Characterization of the plasma plume and of thin film epitaxially produced during laser ablation of SnSe, Appl. Surf. Sci. 90 (1995) 505-514.

[8] N.D. Boscher, C.J. Carmalt, R.G. Palgrave, I.P. Parkin, Atmospheric pressure chemical vapour deposition of SnSe and SnSe 2 thin films on glass, Thin Solid Films 516 (2008) 4750–4757.

[9] S. Sagadevan, Semiconductor Nanomaterials, Methods and Applications: A Review, Nanosci. Nanotechnol. 3(3), (2013) 62-74.

[10] S.M. Ali, J. Muhammad, S.T. Hussain, S.A. Bakar, M. Ashraf, Study of microstructural, optical and electrical properties of Mg dopped SnO thin films, Mater. Sci. Mater. Electron. 24(7), (2013) 2432-2437.

[11] Y. Moon, S. Kim, J. Park, The influence of substrate temperature on the properties of aluminum-doped zinc oxide thin films deposited by DC magnetron sputtering, J. Mater. Sci.: Mater. Electron. 17, (2006) 973-977.

[12] NanoScience and Technology: Nanostructured Materials and Their Applications, Ed. S. Logothetidis, (Springer, Berlin, 2012).

[13] Z.L. Wang, W. Wu, Nanotechnology-enabled energy harvesting for self-powered micro-/nanosystems, Angew. Chem. Int. Ed. 51 (2012) 11700-11721.

[14] N.R. Mathews, Electrodeposited tin selenide thin films for photovoltaic applications, Solar Energy 86 (2012) 1010–1016.

[15] F. K. Butt, C. Cao, W. S. Khan, Z. Ali , R. Ahmed, F. Idrees, I. Aslam, M. Tanveer, J. Li, S. Zaman, T. Mahmood, Synthesis of highly pure single crystalline SnSe nanostructures by thermal evaporation and condensation route, Materials Chemistry and Physics 137 (2012) 565-570.